SUB-MM-WAVE TECHNOLOGIES: SYSTEMS, ICS, THZ TRANSISTORS

M. J. W. Rodwell

Department of Electrical Engineering
University of California, Santa Barbara, CA 93105

Abstract —**mm-wave and sub-mm-wave outdoor communications links have high available bandwidth and can support multiple independent spatial transmission channels but suffer from extremely high worst-case foul-weather attenuation. Link analysis suggests that several useful systems can be realizing using power amplifiers with ~50-200 mW output power, low-noise amplifiers with ~4-7 dB noise figure, and arrays of ~64-128 elements. Such systems can be realized with Si VLSI beamformers, InP HEMT LNAs, and InP HBT or GaN HEMT power amplifiers.**

Index Terms — wireless ICs, bipolar transistors, mm-waves, sub-mm-waves, THz.

I. INTRODUCTION

With progressive scaling of junction dimensions, current densities, contact resistivities, junction thicknesses, and dielectric thicknesses, transistor bandwidths continue to increase. InP HBTs have attained over 1 THz f_{max} [1,2], and >600 GHz ICs [3] have been demonstrated with this technology. InP HEMTs have also attained f_{max} significantly above 1 THz, and, with these, 650 GHz amplifiers [4] have been reported. Even in (32 nm SOI) CMOS VLSI [5], 210GHz transceivers with fundamental have been demonstrated. Research in THz transistors and sub-mm-wave ICs seeks to expand and explore the maximum feasible frequency of operation of electronics, and seeks to develop important applications. Elsewhere we have describe the design and fabrication of THz III-V [6] transistors; here we focus on system design.

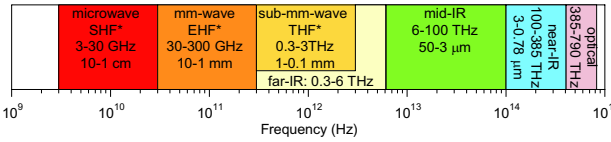

Figure 1: The electromagnetic spectrum from microwave to the visible. Bands* per ITU standard; IR bands per ISO 20473.

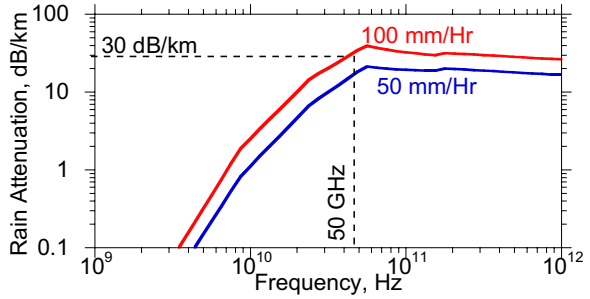

Figure 2: Rain attenuation at 50 mm/hr and 100 mm/hr (exceeded at 10^{-5} probability), calculated from ref. [8]

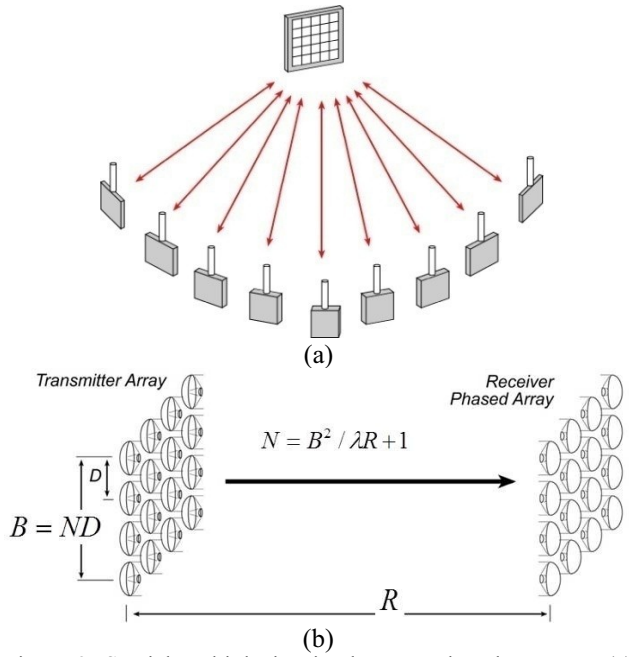

Figure 3: Spatial multiplexing in short-wavelength systems. (a) Phased-array beam steering in a network base station for multiple independent beams at a given carrier frequency. (b) Spatial multiplexing in a line-of-sight mm-wave MIMO link, with the capacity varying as the inverse square of wavelength.

II. MM-WAVE/SUB-MM-WAVE SYSTEMS

Sub-mm-wave and mm-wave (Figure 1) wireless systems can provide very high data capacity. In clear weather, there are large bandwidths at 75-110, 125-165, and 200-300 GHz between absorbtion lines, and narrower bands at higher frequencies. The short wavelengths allow many parallel spatial channels. Phased array base stations (Figure 1a) can provide multiple beams with an angular resolution proportional to λ/(array width). Line-of-sight MIMO links (Figure 1b) provide capacity proportional to $1/\lambda^2$ [7]. Unfortunately, propagation loss is high, both from λ^2/R^2 propagation losses and from foul-weather attenuation. Under 5-9's conditions, rain attenuation [8] is ~30 dB/km from 50-1000GHz, dominating over fog [9] below ~500GHz; 50-500 GHz links must tolerate ~30 dB/km attenuation. Further, the area $\sim \lambda R$ of the first Fresnel zone is small, hence beams are easily blocked. Phased array transceivers are necessary both for adequate transmission range (given the necessary small beam width,

978-1-4799-1472-2/13/$31.00 ©2013 IEEE

fix-aimed antennas are expensive to install) and to provide *adaptive beam steering* in *mesh networks* to accommodate beam blockage.

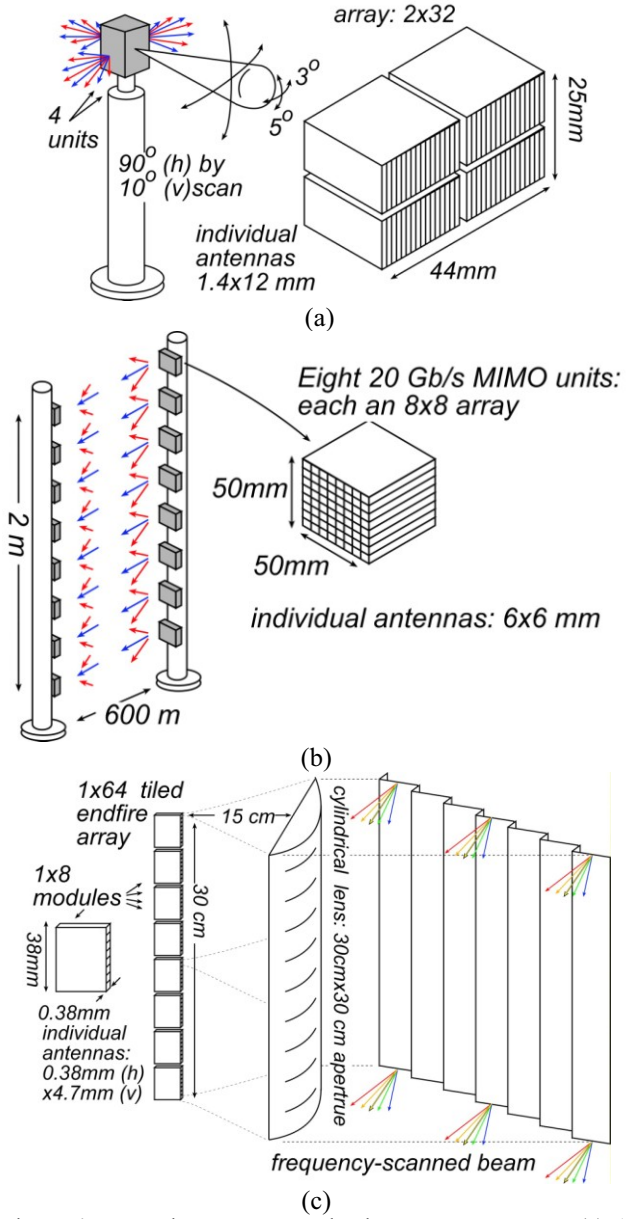

Figure 4: Example mm-wave and sub-mm-wave systems. (a) A 140 GHz, 10 Gb/s adaptive picocell backhaul unit using 64-element arrays . (b) A 340 GHz, 8-channel 160 Gb/s MIMO backhaul link, using 64-element subarray transceivers. (c) A 400 GHz frequency-scanned imaging car radar providing 64x512 elements.

II. Systems Examples

Consider three example systems (Figure 4). The first is a 140 GHz, 10 Gb/s picocell backhaul unit using 64-element arrays. In the event of beam blockage, the arrays steer the transmission to an alternate network node. Given realistic packaging loss, operating & design margins*, power amplifiers (PAs) with $P_{sat} = 24$ dBm per array element, and low-noise amplifiers (LNAs) with F =4 dB, the units can operate over 350 m range (almost two city blocks) in 5-9's rain.

The second is a 340 GHz, 160 Gb/s MIMO backhaul link. This employs a linear 1x8 MIMO superarray, with each element comprised of a 64-element subarray module. Here, given PAs having 24 dbm P_{sat} per element, and LNAs having F =4 dB, range† in 5-9's rain is 600 meters.

The third is a heads-up-display 400 GHz automotive imaging radar, using a linear 1x64 array and frequency-scanned beam steering with a 30cm^2 lens and diffraction grating to form a TV-like picture with 60-Hz-rate, 64x512 pixels, 0.14° resolution, and 10dB-SNR image from a 1 ft^2 target at 300m range in heavy fog. Necessary peak output power is 50mW/element given 6.5dB LNA noise figure‡.

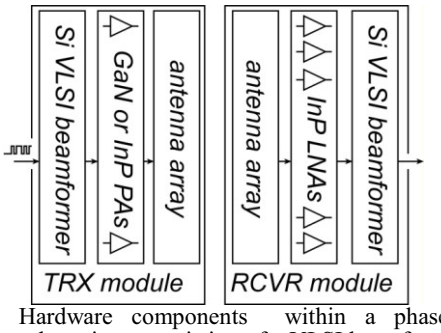

Figure 5: Hardware components within a phased array transmitter and receiver, consisting of a VLSI beamformer, III-V LNAs and PAs, and antenna array.

For these examples, low receiver noise figure and high transmitter output power are necessary for the desired system transmission range. Noting that today's cellular telephones use III-V PAs and LNAs, we suggest that such systems are best realized (Figure 5) with a combination of Si VLSI beam steering ICs and III-V (GaN or InP) PAs and LNAs. ICs can be assembled into phased arrays using Si MEMS wafer-level packaging [10, 11].

In CMOS (sub) mm-wave systems [5], PA output power is lower and LNA noise figure higher than that achievable with III-V technologies. In this case, the necessary system range can be obtained by increasing the number of transmitter and receiver array elements while maintaining fixed the area of an individual element. As the array size increases, directivities increase and both the required per-element transmitter output power and the total required

* Analysis: Propagation loss from the Friis transmission equation, sensitivity from symbol rate assuming lightly-coded QPSK, array directivities from areas. 6dB package loss, 3dB end-of-life, 6dB design margin, 10dB operating margin, 5dB obstruction loss, 5dB PA backoff..

† Analysis: 1° beam width, 8° beam steering, lightly-coded 16QAM, loss & margins similar to example (a).

‡ Analysis: radar range equation, 10dB package loss, 5dB end-of-life, 2% pulse duty cycle, fog @34dB/km.

radiated power deceases. Because power is consumed in signal distribution and phase-shifting, power consumption is high for large arrays, and there is always an intermediate array size which minimizes power consumption. Figure 6 shows calculations for the array of Figure 4a. Low-power phase-shifters and low-power signal distribution are necessary if large arrays are to be viable,

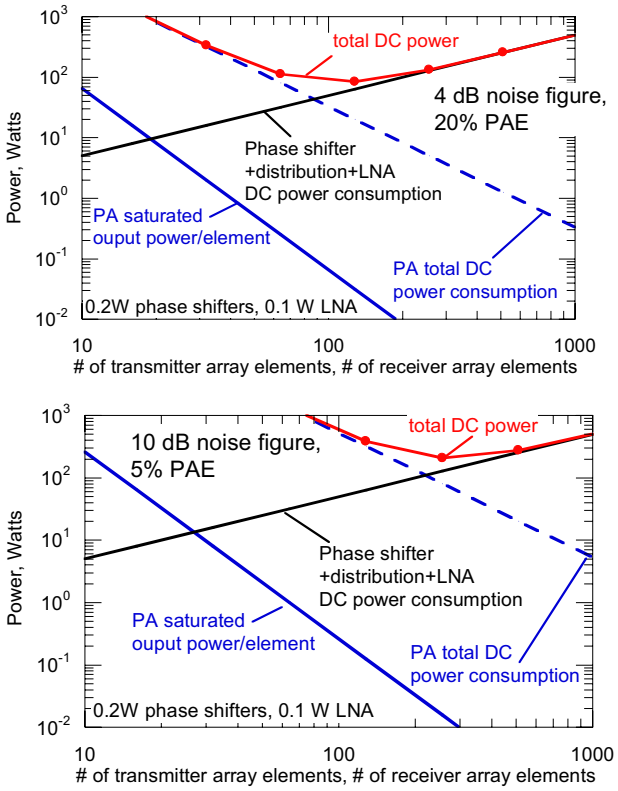

Figure 6: Computed transmitter and receiver power consumption as a function of array size for the system of fig. 4a. As array size increases, required power per PA decreases but power consumed in the beam steering and signal distribution increases.

TRANSISTOR AND IC RESULTS.

Work at UCSB focused on both THz transistor and mm-wave IC development. We will present results on THz InP HBT development at the 130 nm node, with 220 GHz power amplifiers (Figure 7) and phase-shifters, and high-power 85GHz power amplifiers.

ACKNOWLEDGMENT

Portions of this work were performed in the UCSB Nanofabrication Facility, a member of the NSF-funded National Nanofabrication Infrastructure Network. Program support by the DARPA THETA, Hi-Five, and Hotspots programs is acknowledged.

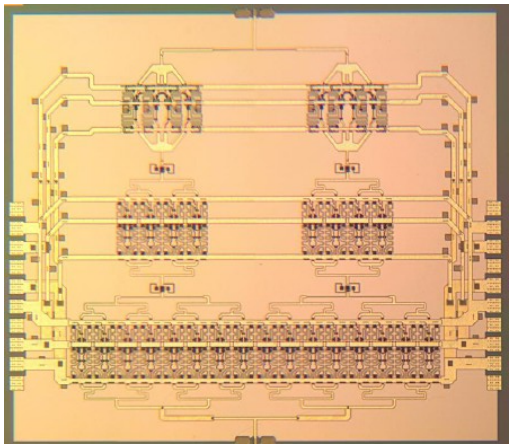

Figure 7: High-power 220 GHz InP Monolithic Power Amplifier. The die is 2.51x2.22mm^2.

REFERENCE

[1] M. Urteaga, R. Pierson, P. Rowell, V. Jain, E. Lobisser, M.J.W. Rodwell, 2011 IEEE Device Research Conference, June 20-22, Santa Barbara

[2] V. Jain, J. C. Rode, H-W. Chiang, A. Baraskar, E. Lobisser, B. J. Thibeault, M. Rodwell, M. Urteaga, D. Loubychev, A. Snyder, Y. Wu, J. M. Fastenau, W.K. Liu, 2011 IEEE Device Research Conference, June 20-22, Santa Barbara

[3] M. Seo, M. Urteaga, J. Hacker, A.Young, A.Skalare, R.Lin, M. Rodwell, 2013 International Microwave Symposium, 2-7 June, Seattle

[4] V. Radisic, K.M.K.H. Leong, X. Mei, S. Sarkozy, W. Yoshida. W.R. Deal, IEEE Trans MTT vol.60, no.3, pp.724,729, March 2012

[5] Zheng Wang, Pei-Yuan Chiang, Peyman Nazari, Chun-Cheng Wang, Zhiming Chen, and Payam Heydari, IEEE Int'l Solid-State Circuits Conference (ISSCC), Feb. 2013

[6] M. J. W. Rodwell, J. Rode, H.W. Chiang, P. Choudhary, T. Reed, E. Bloch, S. Danesgar, H-C Park, A. C. Gossard, B. J. Thibeault, W. Mitchell, M. Urteaga, Z. Griffith, J. Hacker, M. Seo, B. Brar, IEEE Compound Semiconductor Integrated Circuit Symposium (CSICS), 2012 IEEE, San Diego, Oct. 2012

[7] E. Torkildson, U. Madhow, M. Rodwell, IEEE Trans. Wireless Comms., vol.10, no.12, pp.4150-4160, December 2011

[8] R. Olsen, D. Rogers, D. Hodge,.IEEE Trans. Antennas and Propagation, , vol.26, no.2, pp. 318- 329, Mar 1978

[9] H.J Liebe, T. Manabe, G.A. Hufford, IEEE Transactions on Antennas and Propagation, Volume: 37 , Issue: 12 , Dec. 1989

[10] I. Mehdi, G. Chattopadhyay, Choonsup Lee, T. Reck, C. Jung, J. Siles, K. Cooper, N. Llombart, 7th European Microwave Integrated Circuits Conference (EuMIC), pp.230-233, 29-30 Oct. 2012

[11] K.M.K.H. Leong, K. Hennig, Chunbo Zhang; R.N. Elmadjian, Zeyang Zhou, B.S. Gorospe, P.P. Chang-Chien, V. Radisic, W.R. Deal, IEEE Trans. MTT, vol.60, no.4, pp.998,1005, April 2012